

Synthesis, structural studies and photochemistry of cobalt(III) complexes of anthracenylcyclam macrocycles †

Alison M. Funston, Kenneth P. Ghiggino, Martin J. Grannas, W. David McFadyen and Peter A. Tregloan

School of Chemistry, University of Melbourne, Victoria, 3010, Australia

Received 22nd May 2003, Accepted 15th August 2003

First published as an Advance Article on the web 29th August 2003

This work reports the syntheses, structures and some photochemistry in DMF of the cobalt complexes *trans*-[Co^{III}(2)Cl₂]Cl·0.5CH₃OH and *trans*-[Co^{III}(3)Cl₂]Cl·4H₂O, where **2** is 6-(anthracen-9-ylmethyl)-1,4,8,11-tetraazacyclotetradecane-5,7-dione and **3** is 6-(anthracen-9-ylmethyl)-1,4,8,11-tetraazacyclotetradecane. In the preparation of the macrocyclic ligand, **3**, the formation of a polycyclic bis(aminal) intermediate and its subsequent acid hydrolysis to **3** is a cleaner route than the traditional procedure in which the analogous dioxocyclam **2** is reduced with borane reagents. The crystal structure of *trans*-[Co^{III}(3)Cl₂]Cl·4H₂O shows that the macrocycle adopts the *trans*-III conformation, in which the anthracene moiety is extended away from the cobalt ion and the anthracene to Co separation is 7.22 Å. For the related complex *trans*-[Co^{III}(2)Cl₂]Cl·0.5CH₃OH, however, the anthracene is bent over the highly conjugated tetracycle and significant interactions between the anthracene and the complex occur. A novel new complex, *trans*-[Co(12)Cl₂] (where **12** is 5,7-hydroxy-6-oxo-1,4,8,11-tetraazacyclotetradecane-4,7-diene) which is a degradation product of the complex *trans*-[Co^{III}(2)Cl₂]Cl is also reported.

Introduction

Donor–acceptor systems have been reported as models for molecular devices such as photomolecular switches,^{1–3} sensors^{4–9} and machines.⁴ The operation of these relies on variation of the fluorescence quenching properties of the metal and ligands as a function of pH,^{4,5} metal concentration^{6–9} or metal oxidation state.^{1–3} The use of a metal centre as the electron acceptor unit in such systems, the stability of the metal ion in different oxidation states and its distinct properties in those states gives substantial flexibility in the molecular design and diversity of any applications.

A number of the systems developed have made use of quadridentate ligands such as 1,4,8,11-tetraazacyclotetradecane (cyclam)^{4,10} and 1,4,8,11-tetraazacyclotetradecane-5,7-dione,^{7,11} extended and appended to a variety of chromophores including anthracene and naphthalene. Work with these ligands has centred on Ni(II) and Cu(II) complexes and excited state quenching in the metal complexes ascribed to energy or electron transfer processes. The nature of the quenching process has been related to the structure of the spacer between the donor and the metal acceptor groups, although for systems of this type it is still not possible to predict whether an electron transfer or energy transfer mechanism will operate.⁴ Solvent interactions, which may well influence solution conformation, are also likely to play a role in the quenching behaviour of these donor–acceptor systems.¹²

Another potential application of the properties of donor–acceptor systems is their use as tools for triggered ligand release as a model for photoinduced drug delivery. Transient reduction of a stable cobalt(III) acceptor centre to its labile cobalt(II) analogue may provide such a vehicle for controlled ligand release. For this concept to be realised it is important to better understand the nature of the quenching process in donor–acceptor complexes containing cobalt(III) as the acceptor moiety. To this end, and as part of our investigations of photoactivated donor–acceptor complexes we have examined some cobalt(III) complexes of the macrocyclic ligands 6-(anthracen-9-yl)-1,4,8,11-tetraazacyclotetradecane **3** and 6-(anthracen-9-

ylmethyl)-1,4,8,11-tetraazacyclotetra-decane-5,7-dione **2**. In this report we describe the isolation and structural characterisation of the complexes *trans*-[Co^{III}(3)Cl₂]Cl and *trans*-[Co^{III}(2)Cl₂]Cl as well as describing the results of some photochemical investigations of these systems.

Experimental

Electrochemical experiments

Cyclic voltammetry was carried out using a three-electrode cell configuration consisting of a 1 mm glassy carbon disk working electrode, a platinum wire auxiliary electrode, and a Ag/AgClO₄ in [Et₄N]ClO₄ reference electrode separated from the working solution by a liquid junction incorporating a Vycor glass frit. DMF (Merck) was dried over molecular sieves (4Å). [Et₄N]ClO₄ (Fluka) was used as supporting electrolyte and AgClO₄ (BDH) as the source of Ag⁺ in the reference electrode. The ionic strength of the reference electrode was identical to that of the working solution. Formal potentials were determined from the mean of the oxidation and reduction cyclic voltammetric peaks.

Instrumentation

Ultraviolet/visible spectra in DMF were recorded on either a Shimadzu UV-2401PC UV-VIS recording spectrophotometer or Varian Cary 50 Bio ultraviolet-visible spectrophotometer unless otherwise specified. ¹H and ¹³C NMR spectra were measured in d₄-methanol using Varian Unity 300 or Unity Plus 400 spectrometers. Chemical shifts (δ, positive downfield) are given in ppm (methanol reference) and *J* values in Hz.

Photochemistry experiments

Sample preparation. Solutions were prepared in DMF (Merck, spectroscopic grade). In the determination of extinction coefficients, samples were weighed on a Perkin Elmer Autobalance AM-2 to ±5 μg and the optical density (OD) of solutions of known concentration measured using a Cary 50 UV-VIS spectrophotometer. For steady state fluorescence experiments, the OD at 370 nm was adjusted to ~0.1 (corresponding to a concentration of ~0.8–1.0 × 10⁻⁵ M); for flash photolysis experiments, the OD was ~1. Solutions were degassed using multiple freeze–pump–thaw cycles. Typically,

† Electronic supplementary information (ESI) available: Selected bond lengths and angles and ORTEP diagrams for compound **8** and complexes [Co(3)Cl₂]Cl·4H₂O, [Co(12)Cl₂] and [Co(2)Cl₂]Cl·0.5CH₃OH. See <http://www.rsc.org/suppdata/dt/b3/b305773a/>

four cycles were sufficient to remove dissolved gases. Solutions were prepared in the dark and protected from light when not in use.

Steady-state fluorescence. Steady-state fluorescence spectra were recorded using a Varian Eclipse Fluorimeter and corrected for instrumental response. Low-temperature steady-state fluorescence measurements were performed in an ethanol (Merck, spectroscopic grade) glass in cylindrical multichannel cells, using an Oxford Instruments Optistat DN with a liquid nitrogen cryostat. Fluorescence quantum yields were determined by using 9-methylanthracene in ethanol ($\Phi = 0.33$) as the reference.¹³

Time-correlated single photon counting. Fluorescence decay profiles were determined from time-correlated single-photon counting data. The laser excitation source was a jet stream dye laser (Spectra Physics model 3500), synchronously pumped by a mode locked argon ion laser (Spectra Physics model 2030). The output from the DCM dye was set at 700 nm using a 3-plate birefringent filter. The output pulses were pulse-picked and frequency-doubled in a KDP crystal to provide the 350 nm excitation pulses of ~ 5 ps (FWHM) at a repetition rate of 4 MHz. Sample emission was collected through a polarizer set at the magic angle (54.7°) relative to the vertically polarized excitation source. Fluorescence decays were measured at 430 nm using a microchannel plate photomultiplier (Hamamatsu model R2809U-01) interfaced to a 512 channel multichannel analyser and reconvoluted using non-linear least-squares iterative procedures based on the Marquardt algorithm.¹⁴

Flash photolysis. The excitation source in the flash photolysis experiments was a Nd:YAG pulsed laser (Continuum NY-61). The output was frequency tripled to 355 nm to give laser pulses of ~ 7 –8 ns (FWHM) with a pulse intensity limited to ≥ 5 mJ cm⁻² pulse⁻¹. The analysing light source was based on a 150 W xenon arc lamp set perpendicular to the excitation beam. To minimise the effects of excess heating and any UV photo-reaction, the light was passed through UV-cutoff filters (360 or 400 nm as appropriate) and a water bath, prior to the sample solution. The monitoring wavelength was selected using a dual port triple grating monochromator/spectrograph (Acton Research Corporation SpectraPro model 300i). Two optical observation systems were utilised for time resolved optical detection. Kinetic measurements at a single wavelength were detected using a fast response photomultiplier tube (Hamamatsu R928) coupled to a digital recording oscilloscope (Tektronix TDS-520). Transient spectra at specific delay times were collected using a CCD camera (Princeton Instruments I-MAX-512-T ICCD with ST-133 controller).

Steady-state irradiation. 3 mL of a solution containing either [Co(3)Cl₂]Cl ($c = 4.70 \times 10^{-3}$ M) or [Co(2)Cl₂]Cl ($c = 6.42 \times 10^{-3}$ M) in DMF was placed in a glass cuvette and deoxygenated by purging the solution with N₂ for 10 min. The cuvette was capped and sealed using Parafilm then irradiated for 5 h with light from a 100 W high-pressure mercury arc source fitted with a 372 nm narrow bandpass filter. A control solution from the same stock solution was kept in the dark for the duration of the irradiation.

Preparations

Reactions were performed in air using as-received solvents and A.R. reagents unless otherwise specified. Pyridine was dried over 4 Å molecular sieves. 2-(Anthracen-9-ylmethyl)propane-1,3-diol **4**, the bis(aminal) **7** and the ligand 6-(anthracen-9-ylmethyl)-1,4,8,11-tetraazacyclotetradecane-5,7-dione **2** were prepared by literature methods.^{11,15} Elemental analyses were performed by the Microanalytical Laboratory, Department of Chemistry, University of Otago, Dunedin, New Zealand.

2-(9-Anthracenylmethyl)propane-1,3-ditosylate 5. 4-Toluene-sulfonyl chloride (18.5 g, 97.2 mmol) was added in small portions to a rapidly stirred solution of diol **4** (10.00 g, 44.2 mmol) in dry pyridine (50 cm³). After reaction at ambient temperature overnight, the mixture was poured into a slurry of crushed ice in water (0.8 l) and the ditosylate that separated was collected, washed with water, and recrystallised from MeCN. Yield 63%, mp 141–144 °C. ¹H NMR (300 MHz, CDCl₃): δ 8.36 (s, 1H, Ar-10); 8.07–7.97 (m, 4H, Ar-1,4,5,8); 7.64 (d, 4H, *J* 8.2, tosyl); 7.50–7.43 (m, 4H, Ar-2,3,6,7); 7.24 (d, 4H, *J* 8.2, tosyl); 4.00 (d, 4H, *J* 5.3, Ts-CH₂); 3.63 (d, 2H, *J* 8.6, Ar-CH₂); 2.50 (m, 1H, CH); 2.42 (s, 6H, Ar-CH₃).

2-(9-Anthracenylmethyl)-1,3-diiodopropane 6. The crude ditosylate **5** (25.9 g, 45 mmol) was heated at reflux in a solution of sodium iodide (27.0 g, 182 mmol) in acetone (500 ml) for 72 h. After removal of the solvent under reduced pressure, the residue was partitioned between CH₂Cl₂ (300 mL) and water (100 mL). The aqueous phase was extracted with further CH₂Cl₂ (3 \times 100 mL) and the combined organic phases were dried (MgSO₄), evaporated to dryness, then purified by chromatography on SiO₂ (2 : 1 light petroleum (bp 40–60 °C)–CH₂Cl₂). The most mobile band was collected and the solvent evaporated until a microcrystalline pale yellow solid separated. The solid was collected, washed with light petroleum (bp 40–60 °C) and air dried. Yield 95%, mp 134–136 °C. ¹H NMR (300 MHz, CDCl₃): δ 8.42 (s, Ar-10); 8.28 (d, *J* 8.8, Ar-1,8); 8.04 (d, *J* 8.1 Ar-4,5); 7.59–7.47 (m, 4H, Ar-2,3,6,7); 3.76 (d, *J* 7.1 Ar-CH₂); 3.41 (d, *J* 5.4, CH₂I); 2.04 (m, –CH–).

2-(Anthracen-9-ylmethyl)decahydro-*cis*-10*b*,10*c*-dimethyl-1*H*,6*H*-3*a*,5*a*,8*a*,10*a*-tetraazapyrene 8. A solution of diiodopropane **6** (6.395 g, 13.15 mmol), anhydrous K₂CO₃ (9.09 g, 65.8 mmol) and tricyclic bis(aminal) **7** in dry MeCN (250 mL) was heated at reflux for 26 h, in a flame-dried round-bottomed flask fitted with a CaCl₂ guard tube. The dark reaction mixture was filtered, the filtrate was evaporated under reduced pressure and the residue purified by squat SiO₂ column chromatography. After any unreacted **6** had been eluted with CH₂Cl₂, the band that eluted with Me₂CO and which appeared light blue under 365 nm irradiation was collected. Concentration of this fraction yielded a crude mixture of the *syn* and *anti* isomers of **8** that was further purified by vacuum chromatography through a squat SiO₂ column followed by recrystallisation from acetone. Yield = 3.06 g, 51%. Anal. Calc. for C₂₉H₃₄N₄: C, 79.05; H, 8.23; N, 12.72. Found: C, 78.63; H, 8.03; N, 12.81%. The *anti* isomer is significantly less soluble in common solvents such as CHCl₃ and Me₂CO and was separated by crystallization from the latter.

Anti isomer: mp 217–221 °C. ¹H NMR (400 MHz, CDCl₃): δ 8.30 (s, 1H, Ar-10); 7.95 (d, 2H, *J* 8.4, Ar-1,8); 7.4–7.6 (m, 6H, Ar-2,3,4,5,6,7); 4.82 (t, 1H, *J* 11.8); 4.53 (t, 1H, *J* 13); 4.23 (t, 1H, *J* 10.3); 3.88 (m, 1H); 2.3–3.7 (m, 14H); 1.96 (m, 2H); 1.80 (s, 3H, C–CH₃); 1.48 (d, 1H, *J* 13.9); 1.31 (s, 3H, C–CH₃).

Syn isomer: mp 176–179 °C. Poor solubility in common solvents prevented the detailed analysis of the ¹H NMR spectrum of this isomer. ¹H NMR (400 MHz, CDCl₃): δ 8.30 (m); 7.96 (d, *J* 8.5); 7.4–7.5 (m); 4.45 (m); 4.02 (m); 1.8–3.7 (m); 1.39 (s); 1.25 (m).

6-(9-Anthracenylmethyl)-1,4,8,11-tetraazacyclotetradecane tetrahydrochloride hemihydrate 3·4HCl·0.5H₂O. A mixture of isomers of bis(aminal) **8** (2.00 g, 4.42 mmol) was hydrolysed in aq. HCl (60 ml, 2.0 M) in EtOH (60 ml) heated overnight on a steam-bath. The volatile components were removed under reduced pressure, then the residue was triturated with EtOH and evaporated to dryness again. The residue was washed with cold ethanol, then with Et₂O, to produce a colourless microcrystalline solid. Yield 2.33 g, 97%. Anal. Calc. for C₂₅H₃₈Cl₄

Table 1 Crystallography data

Compound	8	[Co(3)Cl ₂]Cl·4H ₂ O	[Co(2)Cl ₂]Cl·0.5CH ₃ OH	[Co(12)Cl ₂]
<i>M_r</i>	440.62	645.92	599.84	380.11
Colour	Colourless	Green	Green	Green
Size/mm	0.02 × 0.07 × 0.11 × 0.12	0.05 × 0.09 × 0.37	0.09 × 0.13 × 0.25	0.06 × 0.06 × 0.09
Lattice	Triclinic	Monoclinic	Triclinic	Orthorhombic
Space group	<i>P</i> $\bar{1}$ (no. 2)	<i>P</i> 2 ₁ (no. 4)	<i>P</i> $\bar{1}$ (no. 2)	<i>P</i> <i>n</i> <i>n</i> <i>m</i> (no. 58)
<i>a</i> /Å	9.9553(6)	10.8717(15)	10.408(4)	10.0111(11)
<i>b</i> /Å	11.6873(5)	6.3706(8)	10.8133(8)	14.891(3)
<i>c</i> /Å	12.1534(5)	23.310(5)	12.018(7)	9.692(2)
<i>a</i> °	115.186(4)	90	93.22(3)	90
<i>β</i> °	96.967(4)	91.034(12)	107.21(5)	90
<i>γ</i> °	107.303(5)	90	94.824(15)	90
<i>V</i> /Å ³	1170.35(10)	1614.2(4)	1282.8(9)	1444.8(4)
<i>D_c</i> /g cm ⁻³	1.250	1.329	1.548	1.748
<i>Z</i>	2	2	2	4
<i>μ</i> /mm ⁻¹	0.586	0.818	1.016	12.887
<i>F</i> (000)	476	680	618	780
<i>λ</i> /Å	1.54180	0.71073	0.71073	1.54180
<i>T</i> /K	291(2)	293(2)	150(1)	150(1)
Scan method	<i>ω</i> -2 θ	<i>ω</i> -2 θ	<i>ω</i> -2 θ	<i>ω</i> -2 θ
θ Range/°	4–75	2–25	2–25	5–70
Standards	7200	7200	7200	7200
Decay (%)	0	0	0	–
Data collected	5675	3639	5212	1274
Unique (<i>R_{int}</i>)	4812 (0.0122)	3112 (0.0271)	4505 (0.0592)	1274
Observed ^a	3859	2066	3623	848
<i>R</i> ₁ ^b	0.0443	0.0667	0.0489	0.0854
<i>wR</i> ₂ ^c	0.1263	0.1849	0.1390	0.2470
<i>S</i>	1.052	1.087	1.023	1.040

^a $I \geq 2\sigma(I)$. ^b $R_1 (I \geq 2\sigma(I)) = \sum |F_o| - |F_c| / \sum |F_o|$. ^c wR_2 (all data) = $(\sum w(F_o^2 - F_c^2)^2) / \sum w(F_o^2)^{1/2}$.

N₄·0.5H₂O: C, 55.05; H, 7.21; N, 10.27; Cl, 26.00. Found: C, 54.88; H, 7.14; N, 10.43; Cl, 25.57%.

The hydrochloride was converted to the free base by treatment with aqueous base (NaOH or NH₃) and extraction into CH₂Cl₂. ¹H NMR (400 MHz, CDCl₃): δ 8.32 (s, Ar-10); 8.26 (d, *J* 8.6, Ar-1,8); 7.96 (d, *J* 8.1, Ar-4,5); 7.48–7.40 (m, 4H, Ar-2,3,5,6); 3.56 (d, *J* 7.4, Ar-CH₂); 2.87–2.50 (m, 16H, CH₂N); 2.34 (m, HC(CH₂)₃); 2.13 (br, 4H, NH, exchanges with D₂O addition); 1.68 (m, -CH₂-).

(6-(9-Anthracenylmethyl)-1,4,8,11-tetraazacyclotetradecane)-dichlorocobalt(III) chloride monohydrate. Aqueous NaOH (2.0 mL, 1.0 M, 2.0 mmol) was added to a hot solution of CoCl₂·6H₂O (119 mg, 0.500 mmol) and 3·4HCl·0.5H₂O (273 mg, 0.500 mmol) in MeOH (40 mL). The pale red–brown solution was heated at reflux overnight, then treated with 2.0 M aqueous HCl (2.0 mL, 4.0 mmol). After a few min cooling, air was bubbled into the mixture for 0.5 h whereupon the mixture rapidly became deep green. The solvent was then boiled off cautiously on a steam-bath, with the occasional addition of small portions (*ca.* 0.5 mL each) of water. When the mixture had been concentrated to *ca.* 10 mL, it was placed in a screw-capped glass jar containing water, which diffused slowly into the mixture with concomitant MeOH diffusion into the water from the reaction mixture. The green microcrystalline solid began separating within 30 min and was collected after 3 days, washed with a minimum of cold water, then dried *in vacuo* at 80 °C for 2 h. Yield = 153 mg, 60%. Anal. Calc. for C₂₅H₃₄Cl₃CoN₄·H₂O: C, 52.32; H, 6.32; N, 9.76; Cl, 18.53. Found: C, 52.44; H, 6.56; N, 9.67; Cl, 18.36%. Visible λ_{\max} : 626 nm, ϵ_{\max} : 33.2 L mol⁻¹ cm⁻¹. ¹H NMR (300 MHz, d₄-MeOH): δ 8.46 (s, Ar-9); 8.32 (d, *J* 8.7, Ar-1,8); 8.06 (d, *J* 8.1, Ar-4,5); 7.59–7.46 (m, 4H, Ar-2,3,6,7); 6.22 (br, 2H, NH); 6.11 (br, 2H, NH); 3.70 (d, *J* 7.5, Ar-CH₂).

(6-(Anthracen-9-ylmethyl)-1,4,8,11-tetraazacyclotetradecane-5,7-dione)dichlorocobalt(III) chloride·0.5CH₃OH. A solution of CoCl₂·6H₂O (167 mg, 0.704 mmol) in ethanol (10 mL) was added to a solution of 6-(anthracen-9-ylmethyl)-1,4,8,11-tetraazacyclotetradecane-5,7-dione **2** (262 mg, 0.627 mmol) in etha-

anol (400 mL). Air was bubbled through the solution for 5 h and the light green solution was then filtered. Upon the slow addition of concentrated hydrochloric acid (2 mL) the solution became dark green. The solvent was evaporated under reduced pressure to a volume of 5 mL during which time a dark green crystalline solid formed. After cooling at -20 °C for 12 h the product was collected and washed with ice-cold ethanol (5 × 1 mL). The product was recrystallised from the minimum amount of 0.67% v/v concentrated HCl–methanol, washed with ice-cold methanol (5 × 1 mL) and dried *in vacuo* at 110 °C for 8 h to yield [Co(6-(anthracen-9-ylmethyl)-1,4,8,11-tetraazacyclotetradecane-5,7-dione)Cl₂]Cl·0.5CH₃OH. Yield = 90 mg, 24%. Anal. Calc. for C₂₅H₃₀Cl₃CoN₄O₂·0.5CH₃OH: C, 51.06; H, 5.38; N, 9.34; Cl, 17.73. Found: C, 51.18; H, 5.58; N, 9.20; Cl, 17.51%. ESI-MS data: parent ion *m/z* 549.5, 547.8. Visible λ_{\max} : 678 nm, ϵ_{\max} : 69 L mol⁻¹ cm⁻¹. ¹H NMR (400 MHz, d₄-MeOH): δ 8.63 (d, *J* 8.6, 2H, Ar CH); 8.49 (s, 1H, Ar CH); 8.07 (d, *J* 9.0, 2H, Ar CH); 7.51 (m, 4H, Ar CH); 6.34 (br, 2H, NH); 4.57 (d, *J* 7.7, 2H, Ar-CH₂); 4.17 (t, *J* 7.5, 1H, cyclam CH); 3.80 (dd, *J* 13.4, 4.4, 2H, cyclam CH); 3.00–3.45 (m, 4H, cyclam CH); 2.63 (d, *J* 11.9, 2H, cyclam CH); 2.20 (d, *J* 15.4, 1H, cyclam CH); 2.00 (q, *J* 15.6, 1H, cyclam CH).

Crystallography

Crystal data and details of data collection and refinement are given in Table 1.

Crystals of [Co(3)Cl₂]Cl·4H₂O suitable for X-ray structure determination were grown by H₂O diffusion into a MeOH solution of the complex. Data were collected on the crystal mounted in a sealed capillary tube in the presence of mother-liquor. Crystals of the (bis-aminal) *anti*-isomer suitable for X-ray structure determination were grown by evaporation from Me₂CO solution and data were collected from the crystal mounted on a glass fibre at room temperature. Single X-ray quality crystals of [Co(2)Cl₂]Cl·0.5CH₃OH were grown by the slow diffusion of acetone into a solution of the complex in methanol containing two drops of trimethylorthoformate. Single X-ray quality crystals of [Co(12)Cl₂] were grown by the

slow evaporation of a solution of (6-(anthracen-9-ylmethyl)-1,4,8,11-tetraazacyclotetradecane-5,7-dione)dichlorocobalt(III) chloride–0.5CH₃OH in methanol over a number of months. The single crystals of [Co(2)Cl₂]Cl·0.5CH₃OH and [Co(12)Cl₂] were mounted on glass fibres, covered in low temperature oil, and kept at 150 K during data collection.

Accurate unit cell parameters were calculated using a least-squares procedure from the setting angles of 25 reflections. Intensity data were collected on an Enraf-Nonius CAD4-MachS single crystal X-ray diffractometer. For [Co(12)Cl₂] during the data collection the cryostat failed, resulting in a time during which the crystal was at room temperature and some solvent lost; as a result of this the intensities of the remaining peaks collected were lower and the peaks broader. The data collection could not be repeated due to the lack of another suitable crystal. Corrections were applied for Lorentz and polarization effects as well as for absorption, the corrections being evaluated by Gaussian integration.

The structures were solved using a combination of direct methods and difference synthesis.^{16,17} The site of the solvent molecule in [Co(2)Cl₂]Cl·0.5CH₃OH was found to be partially occupied and was thus given a refineable occupancy factor. Due to the disorder of the molecule no attempt was made to model attached hydrogen atoms. For [Co(12)Cl₂] the lattice solvent molecule was also disordered and was included in the refinement as an oxygen atom; no attempt was made to model attached atoms. Protons bonded to the oxygen atoms were able to be located using difference synthesis. These were modelled and refined using a 50% occupancy for each of the protonation sites. The structures were refined using a full-matrix least-squares procedure based on F^2 . Hydrogen atoms were located from the difference map and were constrained to geometrical estimates. Final refinement was carried out with anisotropic displacement parameters applied to all non-hydrogen atoms for [Co(2)Cl₂]Cl·0.5CH₃OH. For [Co(12)Cl₂] anisotropic displacement parameters were applied to all non-hydrogen atoms except the solvent molecule which, along with the hydrogen atoms, were refined using isotropic displacement parameters. A weighting scheme of type $[\sigma^2(F_o^2) + (aP)^2 + bP]^{-1}$ was used.

The atomic scattering factors were those incorporated in the SHELXL-97 program system.¹⁷ Calculations were carried out on a Vaxstation 4000VLC computer system. The Figures of the cations and unit cells were prepared from the output of ORTEPIII for Windows.¹⁸

CCDC reference numbers 211119–211122.

See <http://www.rsc.org/suppdata/dt/b3/b305773a/> for crystallographic data in CIF or other electronic format.

Results and discussion

Syntheses of anthracenyl cyclam ligands and complexes

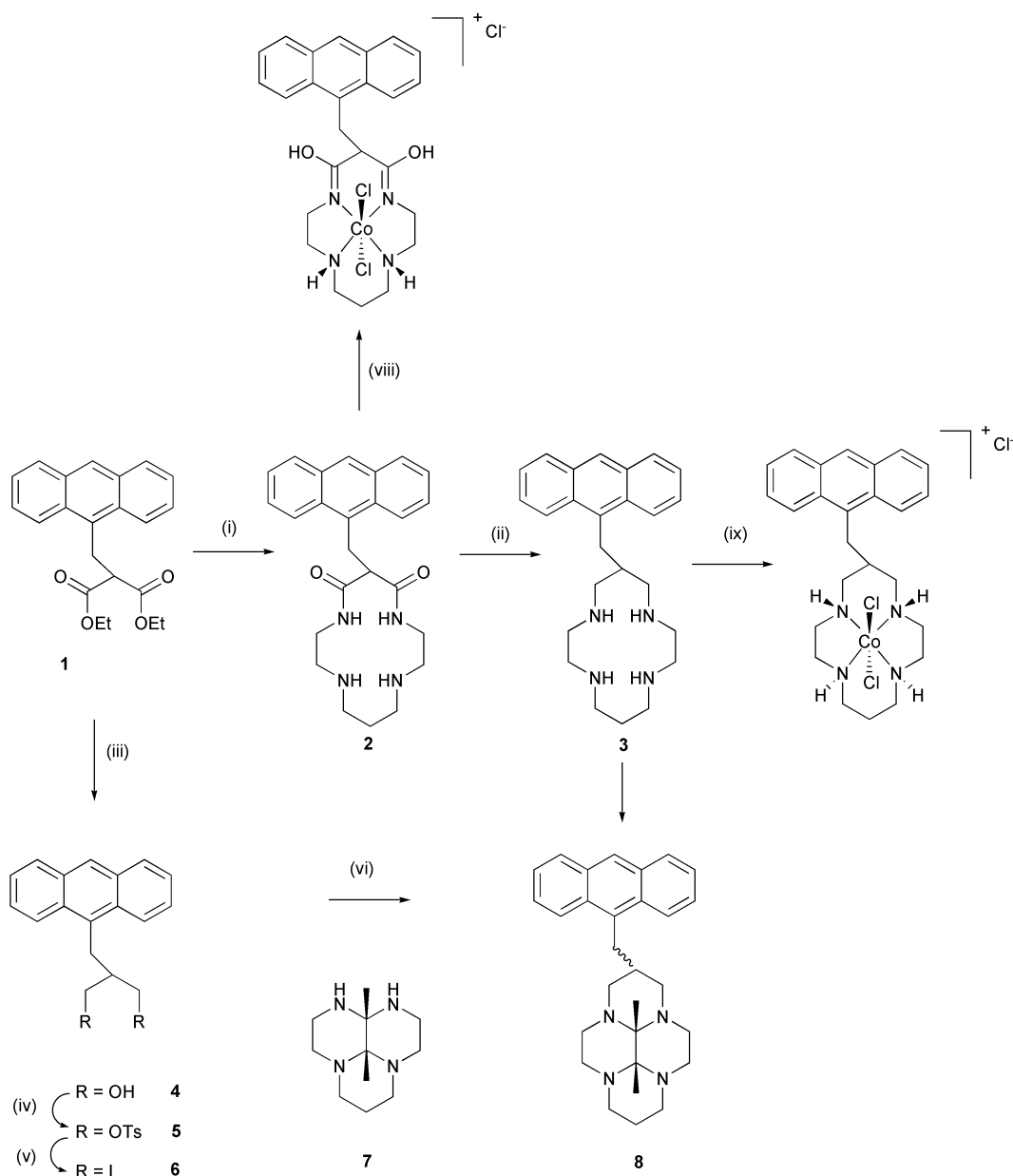
The anthracene-appended macrocyclic ligands were prepared by the routes outlined in Scheme 1. The diamido-diamino macrocycles (**2**) that can be prepared from aminolysis of suitable malonate diesters (**1**) initially seemed to be suitable precursor compounds. This is the “standard” procedure for preparing such C-alkylated macrocycles.¹⁹ Reduction of the amide groups of dioxocyclam **2** using an excess of borane: methyl sulfide complex in THF did not furnish the desired anthrylmethylcyclam **3** cleanly. ¹H NMR analysis of the products of several reduction attempts, performed under a variety of conditions, indicated that the 1,4,8,11-tetraazacyclotetradecane (hereafter cyclam) salt (and its free base) obtained was at best about 80% pure. We were unable to identify or remove the contaminating byproducts. An alternative route to the synthesis of these cyclams was thus investigated.

A recent report described the alkylation of the bis-aminal **7** (formed by condensation of 1,9-diamino-3,7-diazacyclononane (2,3,2-tet) with 2,3-butanedione¹⁵) with 1,3-dibromopropane to

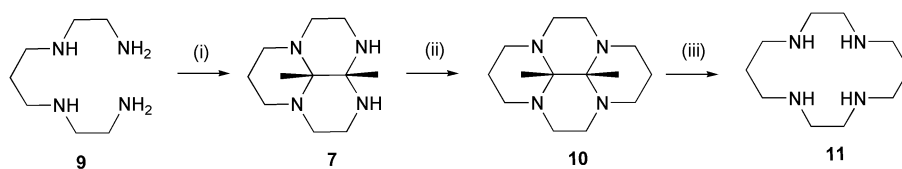
form the dimethyldecahydrotetraazapyrene **10**, which was subsequently hydrolysed to form cyclam **11** in high overall yield as presented in Scheme 2.¹⁵ This prompted us to investigate cognate alkylations using suitably 2-substituted 1,3-diacetated propane derivatives. The desired anthrylmethylpropane was prepared from the known diol **4**, which was converted to the diiodopropane **6** via the ditosylate **5**. Significantly lower cyclization yields were obtained from the reaction of **5** with **7**. The anthracenylmethyl bis-aminal **8** was purified by chromatographic workup. It eluted as a mixture of what we believe to be a mixture of its *syn* and *anti* isomers, which differ in the orientation of the anthracenylmethyl moiety relative to the butanedione-derived methyl groups of the decahydrotetraazapyrene moiety. The single crystal X-ray structure of the *anti* isomer was determined, and confirms the macrocyclic nature of the product. Upon hydrolysis in HCl–H₂O–EtOH solution both proposed isomers yielded 6-anthracenylmethylcyclam **3** as its stable tetrahydrochloride salt. The free base of **3** could be extracted into CH₂Cl₂ from aqueous solutions of 3·4HCl that had been treated with base (e.g. NaOH or NH₃).

Cobalt(III) complexes of **3** were prepared by neutralizing a hot methanol solution of CoCl₂·6H₂O and the tetrahydrochloride of **3** with NaOH solution. A long reaction time allowed the complex to isomerize to its thermodynamically stable state under the neutral to basic conditions where macrocyclic Co–N bonds, and thus conformational inversions, are more labile.²⁰ Subsequent acidification and oxidation allowed the isolation of the cobalt(III) complex. The elemental analysis is consistent with the formation of a clearly defined, pure product which exists as the monohydrate in the crystalline form. Of the many isomers possible, the equatorial *trans*-III isomer (see crystal structure description below) crystallizes from the reaction mixture in better than 90% isomeric purity, determined from the ¹H NMR spectrum of a CD₃OD solution of the product, together with some of the axial *trans*-III isomer. The equatorial *trans*-III isomer obtained by the method described exhibits a characteristic chemical shift (δ 3.70) for the methylene group that links the anthracene to the cyclam, the axial isomer has this group at δ 3.97. Other peaks of low peak area integration “shadow” the aromatic signals of the more abundant isomer. A shorter reaction time always resulted in the final product consisting of an even more complex mixture of other conformations of the Co(III) complex, manifested by lower yields of the characterized isomer, the appearance of other Ar–CH₂ signals, and concomitant additional complexity in both the aromatic and aliphatic regions of the ¹H NMR spectrum.

The *trans*-dichlorocobalt(III) complex of 6-(anthracen-9-ylmethyl)-1,4,8,11-tetraazacyclotetradecane-5,7-dione **2** was prepared in methanol by formation of the Co(II) complex *in situ*, followed by the aerial oxidation of the Co(II) complex to form the Co(III) complex. The product was isolated from an acidic solution and recrystallised from acidified methanol to yield the complex [Co(2)Cl₂]Cl·0.5CH₃OH. Despite drying for prolonged periods at 100 °C *in vacuo* the elemental analysis revealed the presence of a half mole equivalent of solvate, which was masked in the ¹H NMR spectrum by the solvent (d₄-methanol) resonance. The same behaviour was observed when the complex was recrystallised from ethanol, indicating the presence of inaccessible voids in the solid state structure. A single resonance, split into a doublet, is present in the ¹H NMR spectrum at δ 4.57 ppm due to the protons of the methylene bridge. This is in accordance with the symmetry of the complex and indicates the formation of only one isomer of the complex. Puckering of the six-membered chelate ring incorporating C(13) leads to an inequivalence of the C(13) protons. The multiplets at δ 2.20 and 2.00 ppm, each integrating to one proton, are assigned to these protons. The IR spectrum of this complex is consistent with the ligand in the complex existing as the doubly protonated iminol tautomeric structure. The position of the carbonyl stretch of the ligand when complexed to



Scheme 1 Reagents and conditions: (i) 2,3,2-tet, EtOH; (ii) $\text{BH}_3\cdot\text{SMe}_2$, THF; (iii) LiAlH_4 , Et₂O; (iv) TsCl, pyridine; (v) NaI, acetone; (vi) reagent 7, K_2CO_3 , MeCN; (vii) aq. HCl, EtOH; (viii) $\text{CoCl}_2\cdot 6\text{H}_2\text{O}$, EtOH, air, then HCl; (ix) $\text{CoCl}_2\cdot 6\text{H}_2\text{O}$, NaOH, air, then HCl.



Scheme 2 Reagents and conditions: (i) MeCOCOMe , CH_3CN , -7°C , 2 h; (ii) $\text{BrCH}_2\text{CH}_2\text{Br}$, K_2CO_3 , CH_3CN , 60°C , 6 h; (iii) HCl, EtOH, 60°C , 48 h.

the metal (compared to that of the free ligand) has been used as an indicator of the structure and protonation state adopted by ligands containing the 5,7-dioxo functionalisation.²¹ The free ligand, 6-(anthracen-9-ylmethyl)-1,4,8,11-tetraazacyclotetradecane-5,7-dione **2**, displays a carbonyl stretch at 1665 cm^{-1} . The carbonyl stretch of the corresponding cobalt(III) complex, $[\text{Co}(\mathbf{2})\text{Cl}_2]\text{Cl}\cdot 0.5\text{CH}_3\text{OH}$, appears in the IR spectrum at 1701 cm^{-1} . The large frequency increase to 1700 cm^{-1} of this stretch upon complexation to cobalt(III) is characteristic of the formation of a doubly protonated iminol tautomeric structure.²¹ The formation of the iminol tautomer is also consistent with the multiplet at $\delta\ 6.34$ ppm observed in the ^1H NMR spectrum which integrates to two protons and is assigned to the amine protons of N(1) and N(11). The ESI-MS spectrum of the

complex showed the parent ion at $m/z\ 549.5$ and 547 and the isotopic distribution expected for an ion containing ^{35}Cl and ^{37}Cl . Peaks are also observed at $m/z\ 511.5$ and 475.6 consistent with the loss of one and two axially coordinated chloride ligands, respectively, in addition to one or two protons to balance the charge.

Crystal structures

The tetracyclic bis(aminal) **8** crystallizes without lattice solvent from acetone: the solid-state structure determined from a single crystal X-ray study is depicted in Fig. 1 and shows the *anti* disposition of the anthrylmethyl moiety with respect to the butanedione-derived methyl groups. In the solid state the

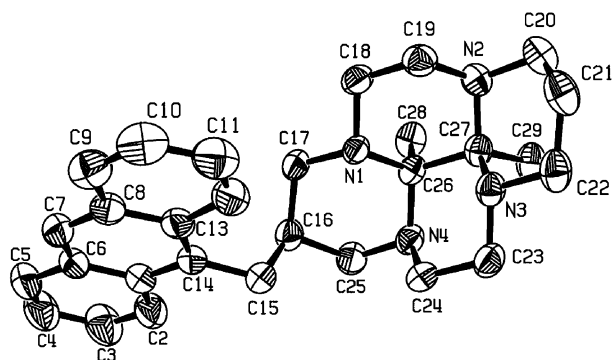


Fig. 1 Diagram of the solid-state structure of **8**. Ellipsoids are scaled to encompass electron density at the 50% probability level. Hydrogen atoms have been omitted.

aromatic anthracene moiety is bent away from the dimethyl-decahydrotetraazapyrene framework although a slight twist across the linking methylene bridge is present and C(17) and C(12) approach to within 3.5 Å of one another. The methyl groups of the dimethyldecahydrotetraazapyrene skeleton exist in the *cis*-configuration, this configuration along with the folding of the decahydrotetraazapyrene framework (due to each of the six-membered rings adopting a chair conformation) has been reported for the non-methyl substituted derivatives.^{15,22} The twisted chiral molecule comprises the asymmetric unit of the structure, but the centrosymmetric structure contains a racemic mixture of both diastereoisomers. The central cross-linking ethylene bridge has a torsion angle of $-47.75(13)$ (for C(28), C(26), C(27), C(29)). Three-dimensional stacking is driven by aromatic coplanar interactions which occur with plane \cdots plane distances of *ca.* 4.2 Å.

The cation in the solid-state structure of *trans*-[Co(3)Cl₂]Cl·4H₂O is depicted in Fig. 2. The Co–N and Co–Cl bond lengths and angles of the slightly distorted octahedra are essentially identical to those of the unelaborated [Co(cyclam)Cl₂]Cl complex.²³ The chloride ligands are coordinated to the cobalt in the *trans*-axial positions and the macrocycle adopts the *trans*-III configuration, with the anthracenylmethyl group occupying an equatorial orientation in the six-membered chair-conformed chelate ring. The anthracene moiety is extended well away from the cobalt cyclam system and does not come in close contact with the atoms of the cyclam macrocycle or cobalt(III) ion. The distance from the centre of the middle anthracene ring to the cobalt atom is significantly greater than that found for *trans*-[Co(2)Cl₂]Cl, being 7.22 Å. The complexes within the unit cell are stacked so that the anthracene chromophores lie directly above one another and the cobalt ions also lie directly above one another. The chloride ligands of one complex are within hydrogen bonding distance of the nitrogen atoms of complexes lying directly above and below the cobalt ion. There are few hydrogen bonding contacts to lattice water, which is highly

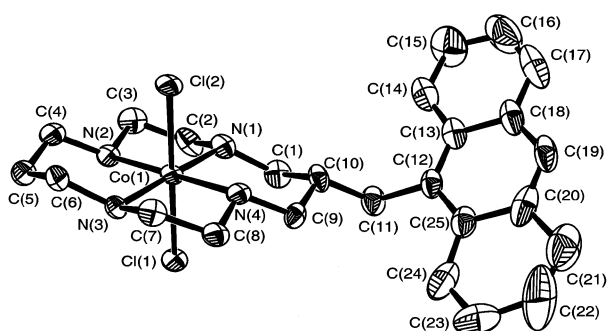


Fig. 2 Diagram of the cation in the crystal structure of *trans*-[Co^{III}(3)Cl₂]Cl·4H₂O. Ellipsoids are scaled to encompass electron density at the 35% probability level. Hydrogen atoms have been omitted.

disordered as a result. Hydrogen bonding contacts between the chloride ligands and the nitrogen atoms of the macrocyclic skeleton link lying to the chloride and lattice water. Significant aromatic coplanar interactions do not occur in the three-dimensional lattice.

¹H NMR experiments indicated that the complex [Co(2)Cl₂]Cl·0.5CH₃OH was stable in methanol for a period of at least 2 days. However, in one attempt to grow crystals suitable for single crystal X-ray diffraction studies, a solution of this complex in d₄-methanol was allowed to evaporate in the dark over a period of some months during which time emerald green crystals were deposited. An X-ray diffraction study of a representative crystal indicated the formation of a novel, and previously unreported, Co(III) complex containing the highly conjugated macrocyclic ligand 5,7-hydroxy-6-oxo-1,4,8,11-tetraazacyclotetradecane-4,7-diene **12** as shown in Fig. 3. The growth of crystals of [Co(2)Cl₂]Cl·0.5CH₃OH suitable for diffraction studies was accomplished by the addition of trimethyl-orthoformate to a solution of [Co(2)Cl₂]Cl·0.5CH₃OH and using diffusion techniques instead of evaporative. Selected bond lengths and angles for the compound **8** and complexes [Co(3)Cl₂]Cl·4H₂O, [Co(12)Cl₂] and [Co(2)Cl₂]Cl·0.5CH₃OH are provided as ESI. † Diagrams of [Co(12)Cl₂] and the cation of [Co(2)Cl₂]Cl·0.5CH₃OH are shown in Figs. 4 and 5.

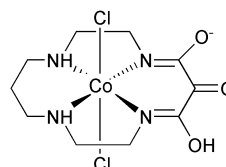


Fig. 3 Structure of *trans*-[Co^{III}(12)Cl₂]

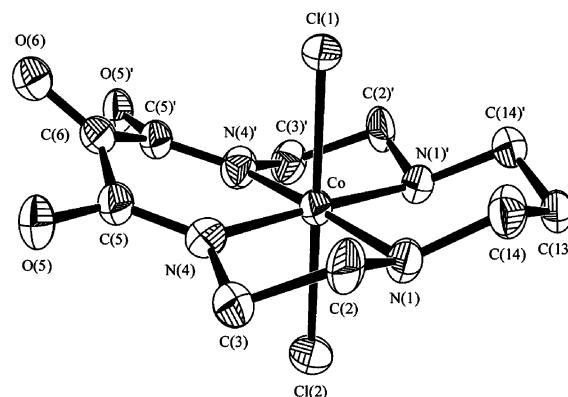


Fig. 4 Diagram of solid-state structure of *trans*-[Co^{III}(12)Cl₂]. Ellipsoids are scaled to encompass electron density at the 50% probability level. Hydrogen atoms have been omitted.

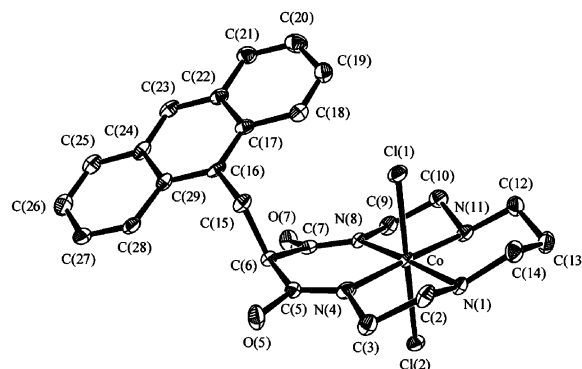


Fig. 5 Diagram of the cation in the crystal structure of *trans*-[Co^{III}(2)Cl₂]Cl·0.5CH₃OH. Ellipsoids are scaled to encompass electron density at the 50% probability level. Hydrogen atoms have been omitted.

The crystal structure of $[\text{Co}(\mathbf{12})\text{Cl}_2]$ is interesting in a number of respects. The complex exists in the iminol tautomeric form, however only one of the oxygen atoms is protonated so that the ligand has a single negative charge. As the cobalt(III) complex also contains two *trans*-diaxial chloride ligands, the overall charge of the complex is neutral. The complex crystallises in the *N-meso* isomeric form with both of the amine protons on the same side of the plane defined by the macrocycle. The crystal packing of $[\text{Co}(\mathbf{12})\text{Cl}_2]$ is driven by close contact hydrogen bonding between the protonated iminol oxygen atom of one cation with the deprotonated iminol oxygen atom of a neighbouring cation. This hydrogen bond has an O–H \cdots O angle of $155(17)^\circ$. The ketone oxygen atom (O(6)) is bent towards N(1) of an adjacent complex, forming a weak hydrogen bond with an O–H \cdots O angle of $121(16)^\circ$. In addition to these, close hydrogen bonding contacts between N(1) and O(5) of a symmetry-related complex are observed. The chloride ligands form no hydrogen bonding contacts and the solvent molecules align in channels throughout the cation network.

Within the complex, the cobalt atom lies within a slightly distorted octahedral coordination environment. The Co–Cl bond lengths and bite angles of the ethylene ($85.6(3)^\circ$) and propylene bridges ($94.9(4)$ and $93.8(4)^\circ$) are typical of those found for related complexes. The Co–N_{imine} bond lengths ($1.907(8)$ Å) are similar to those found in cobalt(III) complexes containing derivatives of 5,7-dioxo-1,4,8,11-tetraazacyclotetradecane lacking the oxo-group at C6²¹ as well as $[\text{Co}(5,7\text{-dimethyl-6-oxo-1,4,8,11-tetraazacyclotetradeca-4,7-diene})\text{Cl}_2]\text{ClO}_4$.²⁴ It is noteworthy that none of these systems display the same degree of conjugation as found in $[\text{Co}(\mathbf{12})\text{Cl}_2]$. The highly conjugated ring containing Co, N(4), C(5), C(6), C(7) and N(8) is distorted from planarity and adopts a boat-like conformation. O(5) and O(7) are bent 0.2198 Å below the plane defined by this ring whilst O(6) is bent significantly above the plane, 0.7240 Å. These trends are similar to that found for the related complex $[\text{Co}(5,7\text{-dimethyl-6-oxo-1,4,8,11-tetraazacyclotetradeca-4,7-diene})\text{Cl}_2]\text{ClO}_4$,²⁴ which also contains a ketone at C(6). It has been postulated that oxidation at the C(6) position may lead to a reduction in the strain of the macrocycle²⁴ which may result in a driving force for the decomposition of the cobalt(III) tethered complex to this novel species.

The cyclam ligand backbone of $[\text{Co}(\mathbf{12})\text{Cl}_2]$ may also be compared to that determined for the anthracene tethered cobalt(III) complex, $[\text{Co}(\mathbf{2})\text{Cl}_2]\text{Cl}$. The crystal structure of $[\text{Co}(\mathbf{2})\text{Cl}_2]\text{Cl}$ reveals that this complex is isolated in the iminol form, although, in contrast to $[\text{Co}(\mathbf{12})\text{Cl}_2]$, both of the oxygen atoms are protonated and the ligand is neutral. The sp^3 hybridised nitrogen atoms, N(1) and N(11), of $[\text{Co}(\mathbf{2})\text{Cl}_2]\text{Cl}$ are also in the *N-meso* isomeric form.

The cobalt(III) atom in $[\text{Co}(\mathbf{2})\text{Cl}_2]\text{Cl}$ lies slightly out of the least squares plane ($0.1484(11)$ Å) of the macrocyclic ligand. The coordination sphere is slightly distorted from ideal octahedral geometry due to the restrictions imposed by the five- and six-membered chelate rings of the macrocycle. The observed bond lengths and bite angles of the macrocyclic ligand are essentially identical to those found for related complexes containing the 5,7-dioxo functionality^{21,24} as well as $[\text{Co}(\mathbf{12})\text{Cl}_2]\text{Cl}$. In contrast to the solid-state structure observed in the corresponding four-coordinate nickel(II) complex,¹¹ for $[\text{Co}(\mathbf{2})\text{Cl}_2]\text{Cl}$ the appended anthracene moiety is not folded over the top of the metal atom but is extended away from the macrocycle. Despite this, however, a small rotation about the C(6)–C(15) bond is present leading to a torsion angle of $54.4(4)^\circ$ for C(7)–C(6)–C(15)–C(16). This results in the anthracene ring atoms C(16), C(17), C(18) and C(19) lying directly over atoms of the macrocycle (C(7), O(7), N(8) and C(9)). The closest approach distance between the anthracene ring and the macrocycle occurs between C(16) and C(7) (3.02 Å) whilst the O(7)–C(16) distance is 3.06 Å. Other approach distances for the atoms listed above are 3.2 – 4.5 Å. The point of closest approach

of the anthracene to the cobalt atom occurs at C(18) and the distance between these two atoms is only 4.65 Å, whilst the distance from the cobalt ion to the centre of the middle anthracene ring is 6.50 Å. The anthracene moiety is essentially planar with the maximum deviation $0.0558(32)$ Å for C(25). The least squares plane of the anthracene is at an angle of $29.14(8)^\circ$ to that of the macrocycle.

Photochemistry

Photochemical investigations on the tethered donor–acceptor complexes $[\text{Co}(\mathbf{3})\text{Cl}_2]\text{Cl}$ and $[\text{Co}(\mathbf{2})\text{Cl}_2]\text{Cl}$ have been carried out and interesting photochemical behaviour is observed. The absorption and emission data for the free ligands **2** and **3** and their corresponding cobalt complexes along with appropriate photophysical data are reported in Table 2. Steady-state fluorescence excitation and emission spectra of **2** and **3** are presented in Fig. 6. The absorption and fluorescence spectra of the metal free ligands display bands characteristic of the anthracene fluorophore.

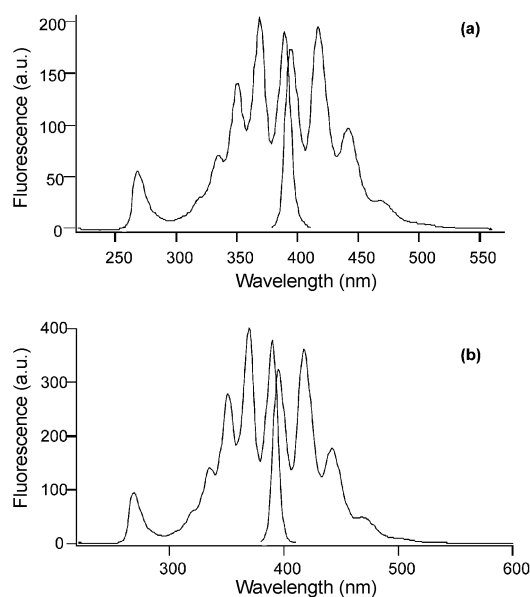


Fig. 6 Steady-state fluorescence excitation and emission spectra of **3** [panel (a)] in DMF and **2** [panel (b)] in DMF.

Incorporation of the cobalt(III) ion into the ligand **2** leads to a significant (approximately 3 nm) red shift of the anthracene absorption bands indicating a ground state interaction between the anthracene moiety and the cobalt ion. An analogous shift has been observed in related nickel(II) complexes.¹¹ In contrast to the square-planer nickel(II) complex, however, for $[\text{Co}(\mathbf{2})\text{Cl}_2]\text{Cl}$ the octahedral geometry of Co(III) and the presence of the axial Cl^- ligands hinders the approach of the anthracene to the cobalt(III) ion. Despite this, the red shift indicates some interaction of the aromatic anthracene rings with a highly conjugated section of the macrocycle does occur, as shown by the single-crystal X-ray diffraction studies. It is likely to be this interaction between the anthracene and the orbitals of the acceptor unit that causes the observed red shift in the anthracene bands of $[\text{Co}(\mathbf{2})\text{Cl}_2]\text{Cl}$.

The absorption spectrum of the donor–acceptor system $[\text{Co}(\mathbf{3})\text{Cl}_2]\text{Cl}$ does not display a similar shift in the absorbance of the anthracene bands. This is consistent with the fully extended structure existing as the main conformer in solution, as is observed in the solid state, and therefore the lack of interaction between the cobalt ion and anthracene chromophore in the ground state.

Upon complexation of the ligand to cobalt(III), the fluorescence of the anthracene fluorophore is quenched dramatically. The decay of fluorescence of the free ligand **3** did not

Table 2 Photophysical properties of the donor–acceptor systems and the free ligands in DMF

Compound	$\lambda_{\text{max}}/\text{nm}$	$\epsilon_{\text{max}}/\text{M}^{-1} \text{cm}^{-1}$	Emission $\lambda_{\text{max}}/\text{nm}$	Quantum yield	Lifetime(s)/ns
3	369	9250	417	0.15	1.68 (21%), 10.31 (79%)
[Co(3)Cl ₂]Cl	370	9820	^a	<0.01	0.06
2	370	10000	417	0.68	10.57
[Co(2)Cl ₂]Cl	373	11600	^a	<0.01	^a

^a Not measurable.

follow simple first-order kinetics but was comprised of two first-order decay pathways, the major pathway (79%) having a lifetime of 10.31 ns and a minor component (21%) with a lifetime of 1.68 ns. The presence of two lifetimes suggests that there may be two conformational forms of **3** present in the DMF solution, each of which have different energy relaxation pathways. For the ligand **2**, however, the fluorescence decay follows good first-order kinetics to yield a fluorescence lifetime of 10.57 ns.

Complexation of **3** to cobalt(III) results in dramatic quenching of the anthracene fluorescence by the coordinated cobalt ion. However, for [Co(3)Cl₂]Cl fluorescence decay analysis could extract a very rapid major decay component of 0.06 ns corresponding to the presence of an additional non-radiative process with a rate constant of $1.6 \times 10^{10} \text{ s}^{-1}$. For [Co(2)Cl₂]Cl the rate of quenching is too fast to be detected. Metal complexation thus in this case provides an extremely efficient fluorescence quenching pathway within the time resolution of our time-correlated single-photon counting apparatus (<50 ps).

The mechanism of quenching of the anthracene excited state by the cobalt ion may be *via* energy transfer (EnT) or electron transfer (ET) or a combination of both mechanisms. Förster resonance energy transfer (FRET) calculations were carried out for the system [Co(3)Cl₂]Cl using equations (2.16), (2.17) and (2.18) of reference 25 with a J value of $6.369 \times 10^{-17} \text{ M}^{-1} \text{ cm}^3$ and a κ^2 value of 2/3. These calculations indicate that energy transfer between the donor and acceptor is predicted to be efficient (~90%) and rapid ($k_{\text{EnT}} = 9.4 \times 10^8 \text{ s}^{-1}$). This is due to the close proximity (7.22 Å) of the donor to the acceptor, which is well within the calculated Förster distance of 10.6 Å. Although these calculations show that energy transfer in [Co(3)Cl₂]Cl is efficient, the observed quenching is much higher than that predicted to occur by the Förster energy transfer mechanism. Thus the energy transfer mechanism cannot explain all the quenching observed. This difference could be explained by an electron transfer mechanism occurring either solely or in competition with energy transfer. Analogous calculations cannot be carried out for the donor–acceptor system [Co(2)Cl₂]Cl due to the close proximity of the donor to the acceptor and resulting possibility of energy transfer *via* the Dexter mechanism.

The driving force for electron transfer from the donor to the acceptor can be estimated using the Rehm–Weller equation which requires a knowledge of the reduction potentials of the donor and acceptor and the excitation energy of the chromophore.²⁶ In DMF the cyclic voltammogram of the acceptor unit, [Co(cyclam)Cl₂]⁺, shows quasi-reversible oxidation and reduction processes for the Co^{III/II} couple allowing the determination of the half-wave potential as $E_{1/2} = -0.794 \text{ V}$ (with respect to Ag/0.01 Ag⁺). Thus, the free energy change for the electron transfer can be calculated as $\Delta G_{\text{eT}} = -1.19 \text{ eV}$ (based on the experimentally obtained E_{oo} value of 2.973 eV from the λ_{max} emission peak of the free ligand at 417 nm and $E_{1/2}(\text{An}^+/\text{An}) = 0.99 \text{ V}^{27}$), indicating that there is a strong driving force for electron transfer from the donor to the acceptor in this system. For [Co(2)Cl₂]Cl the reduction potential of the acceptor unit, [Co(dioxocyclam)Cl₂]⁺ (dioxocyclam is 1,4,8,11-tetraazacyclotetradecane-5,7-dione), could not be determined in DMF with any certainty. However, based upon data obtained in aqueous solution using both cyclic voltammetry and rotating disk

electrode electrochemistry, the reduction potential of the Co^{III/II} couple of [Co(dioxocyclam)Cl₂]⁺ would be expected to be approximately 100 mV more negative than that of [Co(cyclam)Cl₂]⁺, resulting in a more negative free energy change for the electron transfer from the donor to acceptor in [Co(2)Cl₂]Cl than is calculated for [Co(3)Cl₂]Cl. Hence for both the tethered donor–acceptor systems the electron transfer process is thermodynamically favourable.

Steady-state fluorescence experiments in ethanol glass (at 120 K) for both donor–acceptor complexes studied resulted in no revival of the anthracene fluorescence. Whilst intramolecular electron transfer would be expected to be much more dependent upon solvent interactions than intramolecular energy transfer, the extent of destabilisation of the charge separated state upon electron transfer in a glass and hence recovery of fluorescence, is debatable. Additionally the potential proximity of the donor and acceptor, particularly in the case of [Co(2)Cl₂]Cl, adds a further complication to the interpretation of steady-state glass experiments.

The discussion above indicates that the quenching of the anthracene fluorescence by both energy transfer or electron transfer mechanisms is possible. Flash photolysis experiments were unable to further elucidate the mechanism of quenching as the formation of a charge separated state exhibiting the spectral characteristics of the anthracene cation²⁸ or changes in the Co(III) centred ligand field bands at 678 nm due to the formation of Co(II) were not observed. The lack of any significant transient absorption in the spectra of these complexes indicates that the lifetime of the species produced following either energy or electron transfer from the donor to the acceptor is too short for detection using the flash photolysis equipment employed. The laser pulse used was of the order of 7–8 ns and this sets the upper limit for the detection of short lived transients. Lifetimes of ~4 ns have been observed for the anthryl radical cation in donor–acceptor systems containing polyimides as the acceptor unit.²⁸

The photochemistry of cobalt(III) complexes has been the subject of considerable study in recent years.²⁹ In preliminary experiments with the present cobalt(III) complexes we have shown that irradiation of the compounds at 372 nm in DMF (which corresponds to the anthracene absorption bands) results in a change in the visible absorption spectrum of both compounds [Co(3)Cl₂]Cl and [Co(2)Cl₂]Cl. During the irradiation a noticeable color change in the solutions occurred, consistent with a change in the coordination sphere of the metal ion. For both complexes a shift in the λ_{max} and an increase in the absorbance of the visible d–d band is observed along with the grow in of an additional band. No change is observed over this time in the spectra of the control solutions left in the dark. These observations suggest that a change in the coordination sphere of the cobalt(III) metal ion occurs as a direct result of irradiation. It is known that the aquation of the cobalt(III) acceptor unit of [Co(3)Cl₂]Cl, [Co(cyclam)Cl₂]³⁺ results in an increase in the absorption coefficient around 570 nm as observed here.³⁰ In addition to this, prolonged heating of the acceptor unit of [Co(2)Cl₂]Cl, [Co(O₂cyclam)Cl₂]³⁺ in DMF led to an identical change in the spectrum. It is likely that the change in the absorption spectrum of both complexes is the result of the replacement of the *trans*-diaxial chloride ligands with either

trace amounts of water or DMF and that the irradiation of the complex results in ligand release from the donor–acceptor systems. It is noted that under the same conditions irradiation of the acceptor unit for [Co(3)Cl₂]Cl, [Co(cyclam)Cl₂]³⁺ led to no observable change in the UV-visible spectrum, whilst irradiation of the acceptor unit for [Co(2)Cl₂]Cl, [Co(O₂cyclam)-Cl₂]³⁺ under the same conditions led to a change in the spectrum, with the grow in of a band at $\lambda = 610$ nm and the band at $\lambda_{\text{max}} = 626$ nm shifting to $\lambda_{\text{max}} = 676$ nm along with an increase in its intensity.

Conclusions

Although photo-activated ligand release occurs for the donor–acceptor systems, the mechanism operating is not clear. Electron and energy transfer are possible in the anthracene tethered donor–acceptor systems [Co(3)Cl₂]Cl and [Co(2)Cl₂]Cl and both of these processes could lead to the observed behaviour. To better understand the factors responsible we are presently examining related complexes in which a range of axial ligands are coordinated to a cobalt(III) cyclam moiety tethered to either anthracene and naphthalene donors.

Acknowledgements

We thank the Australian Research Council for financial support. A. M. F. acknowledges the support of an AINSE scholarship. Assistance with the photochemical measurements by Mr Nuno Cabral is gratefully acknowledged. The authors would also like to acknowledge most helpful discussions with Dr Brendan Abrahams concerning X-ray crystallography.

References

- 1 R. Bergonzi, L. Fabbrizzi, M. Licchelli and C. Mangano, *Coord. Chem. Rev.*, 1998, **170**, 31.
- 2 G. D. Santis, L. Fabbrizzi, M. Licchelli, N. Sardone and A. H. Velders, *Chem. Eur. J.*, 1996, **2**, 1243.
- 3 G. D. Santis, L. Fabbrizzi, M. Licchelli, C. Mangano and D. Sacchi, *Inorg. Chem.*, 1995, **34**, 3581.
- 4 V. Amendola, L. Fabbrizzi, M. Licchelli, C. Mangano, P. Pallavicini, L. Parodi and A. Poggi, *Coord. Chem. Rev.*, 1999, **190**, 649.
- 5 L. Fabbrizzi, M. Licchelli, P. Pallavicini and L. Parodi, *Angew. Chem., Int. Ed.*, 1998, **37**, 800.
- 6 L. Fabbrizzi, M. Licchelli, P. Pallavicini, A. Perotti and D. Sacchi, *Angew. Chem., Int. Ed. Engl.*, 1994, **33**, 1975.
- 7 L. Fabbrizzi, M. Licchelli, P. Pallavicini, A. Perotti, A. Taglietti and D. Sacchi, *Chem. Eur. J.*, 1996, **2**, 75.
- 8 L. Fabbrizzi, M. Licchelli, P. Pallavicini, D. Sacchi and A. Taglietti, *Analyst*, 1996, **121**, 1763.
- 9 B. Juskowiak and W. Szczepaniak, *Anal. Chim. Acta.*, 1994, **290**, 121.
- 10 P. V. Bernhardt, E. G. Moore and M. J. Riley, *Inorg. Chem.*, 2001, **40**, 5799.
- 11 S. Boyd, N. M. Cabral, K. P. Ghiggino, M. J. Grannas, W. D. McFadyen and P. A. Tregloan, *Aust. J. Chem.*, 2000, **53**, 651.
- 12 M. R. Wasielewski, *Chem. Rev.*, 1992, **92**, 435.
- 13 C. A. Parker and T. A. Joyce, *Chem. Commun.*, 1967, 744.
- 14 D. V. O'Connor and D. Phillips, *Time Correlated Single Photon Counting*; Academic Press, New York, 1983.
- 15 G. Herve, H. Bernard, N. Le Bris, J.-J. Yaouanc, H. Handel and L. Toupet, *Tetrahedron Lett.*, 1998, **39**, 6861.
- 16 G. M. Sheldrick, *Acta Crystallogr., Sect. A.*, 1990, **46**, 467.
- 17 G. M. Sheldrick, in SHELXL-97, Program for the Refinement of Crystal Structures, University of Göttingen, Germany, 1997.
- 18 L. J. Farrugia, *J. Appl. Crystallogr.*, 1997, **30**, 565.
- 19 I. Tabushi, Y. Taniguchi and H. Kato, *Tetrahedron Lett.*, 1977, **12**, 1049.
- 20 I. I. Creaser, T. Komorita, A. M. Sargeson, A. C. Willis and K. Yamanari, *Aust. J. Chem.*, 1994, **47**, 529.
- 21 A. Jyo, Y. Terazono and H. Egawa, *Anal. Sci.*, 1995, **11**, 51.
- 22 P. Gluzinski, J. W. Krajewski, Z. Urbanczyk-Lipkowska, J. Bleidelis and A. Kemme, *Acta Crystallogr., Sect. B*, 1982, **38**, 3038.
- 23 M. E. Sosa-Torres and R. A. Toscano, *Acta Crystallogr., Sect. C*, 1997, **53**, 1585.
- 24 B. Durham, T. J. Anderson, J. A. Switzer, J. F. Endicott and M. D. Glick, *Inorg. Chem.*, 1977, **16**, 271.
- 25 B. Wieb Van Der Meer, G. Coker III and S.-Y. Simon Chen, *Resonance Energy Transfer Theory and Data*, VCH Publishers, Inc., 1994.
- 26 A. Z. Weller, *Phys. Chem. Neue Folge*, 1982, **130**, 93.
- 27 B. Case, N. S. Hush, R. Parsons and M. E. Peover, *J. Electroanal. Chem.*, 1965, **10**, 360.
- 28 W. Li and M. A. Fox, *J. Phys. Chem. B.*, 1997, **101**, 11068.
- 29 D. M. Roundhill, *Photochemistry and Photophysics of Metal Complexes*, Plenum Press, New York, 1994, pp. 42–49.
- 30 C. K. Poon and M. L. Tobe, *J. Chem. Soc. A*, 1967, 2069.